
Fractional Order Kelvin-Voigt Constitutive Model and Dynamic Damping Characteristics of Viscoelastic Materials

Yuan Qin, Bokai Wang, Yuhui Wang, Yao Wang and Yong Song

School of Vehicle and Transportation Engineering, Taiyuan University of Science and Technology, Taiyuan, CN-030024, China. E-mail: qinyuankd@tyust.edu.cn

Xin Shi

Taiyuan Heavy Industry Co., LTD, Taiyuan 030024, China.

(Received 29 March 2024; accepted 10 October 2024)

Viscoelastic damping materials are often under complex service conditions. To precisely characterize its dynamic damping properties, based on fractional calculus and viscoelastic theory, considering the periodic characteristics of viscoelastic materials, the distributed fractional order Kelvin-Voigt constitutive model (DFKV) was constructed. The model accuracy was validated by quasi-static experiments. The dynamic modulus expressions were derived, and the model parametric feature analysis was carried out. Dynamic Mechanical Analysis (DMA) and Separate Hopkinson Pressure Bar (SHPB) experiments were performed with silicone rubber as the subject. The results show that the silicone rubber has an obvious temperature and frequency dependence, and it has a strong strain rate correlation considering that the strain rate effect indexes that are under high strain is 29.331. At the same time, clearly the viscoelastic dynamic constitutive behavior has phased characteristics that are in line with the scientific assumption of the distribution order. The fitting accuracy of DFKV model is higher than the existing contrast models, which reflects DFKV model and favorably represents the dynamic mechanical properties of viscoelastic materials under wide temperature, frequency and strain rate. The model is highly accurate, has fewer parameters, and the physical meaning of its parameters is clearer. It can provide a theoretical reference for the research and design of viscoelastic damping materials.

1. INTRODUCTION

Viscoelastic damping materials have good energy consumption capacity and relatively low manufacturing and maintenance cost. They are often used as vibration control materials in mechanical equipment, aerospace, bridge and culvert engineering and other fields.¹⁻³ Under the dynamic conditions such as variable temperature, variable frequency and impact, the viscoelastic damping material presents dynamic constitutive mechanical behavior. Accurate and reliable viscoelastic constitutive model is the key basis for modeling, analysis and calculation of a viscoelastic oscillator.

The researchers proposed a series of viscoelastic constitutive models to characterize the constitutive mechanical behavior of materials. The standard rheological model includes Maxwell model and Kelvin-Voigt model. On this basis, the Zener model, Burgers model, generalized Maxwell model and generalized Kelvin-Voigt model are developed.^{4,5} Zener⁶ proposed a complex Zener model for describing the creep and relaxation properties of materials. Scholar Bürgers⁷ constructed the Bürgers model by concatenating the Maxwell and Kelvin-Voigt models. The above models are integer order constitutive models, which have the advantages of simple structure and clear concepts, as well as often being used to describe the linear viscoelastic mechanical behavior.

With the development of the fractional calculus theory, Nutting⁸ and Gemant⁹ first found that the fractional order of material strain was associated with its mechanical properties, and

creatively used the fractional derivatives to describe the constitutive relationship of viscoelastic materials. Koeller¹⁰ proves that the order in the fractional equation can characterizes the change of viscoelastic materials from a solid state to a liquid state. Müller et al.¹¹ introduced evolutionary equations into multiaxial stress states and implemented finite element simulations of iterative linear and nonlinear fractional order viscoelastic models. Khajehsaeid¹² modeled the stress relaxation response under finite deformation conditions and showed that the fractional order principal model requires only three parameters while the integer order model requires five parameters. The fractional formula order differential viscoelastic model can fit the relaxation data with relatively fewer material parameters.

In order to improve the fitting accuracy of the viscoelastic constitutive materials, some scholars have proposed a higher-order fractional derivative model by increasing the number of model configurations and parameters. Note: the highest order is greater than 1 for different values of the parameter. Jianguo¹³ obtained the higher fractional derivative model connected in series or in parallel (FVMS or FVMP) from the fractional order Kelvin-Voigt and Maxwell models in parallel or in series, derived the expressions of the complex modulus and complex flexibility of the material, and qualitatively analyzed the influence of the fractional derivative operator. Yongling¹⁴ added Scott-Blair sticky pot based on the fractional derivative Zener model and proposed a 5-parameter fractional derivative mode-

as well as analyzed the influence of fractional derivative operator parameters on the shape of Cole-Cole curve. Mingyu¹⁵ proposed the generalized fractional element network-Zener viscoelastic constitutive model (GFE-Zener model), added the “coordination equation”, developed the method of discrete seeking inverse Laplace transform, and then expanded the construction of model solutions to the generalized function space, so that it can contain more solutions with obvious physical significance. Due to the global relevance of fractional calculus, the fractional-order constitutive model can reflect the history dependence of the evolution of the mechanical properties of viscoelastic materials and can describe the coexistence of elasticity and viscosity of viscoelastic materials, as well as the dynamic mechanical properties in a certain time-frequency domain.^{16,17}

Viscoelastic damping materials often bear high frequency heavy loading, and their dynamic mechanical properties are clearly different from those at low strain rates. While existing studies on the mechanical properties of viscoelastic materials mainly focus on low strain rate conditions, and are based on static, quasi-static loading and simple harmonic excitation experiments,¹⁸ it fails to reveal the mechanical properties and damping mechanism of viscoelastic materials at high strain rates. The Separate Hopkinson Pressure Bar (SHPB) technique, invented by Kolsky in 1949, is now a classic technique for testing the high strain rate constitutive mechanical behavior of materials.^{19,20} In order to predict the strain rate effect of polymer materials under impact loading, Zhaoxiang et al.^{21,22} proposed the ZWT nonlinear viscoelastic constitutive model for the first time. They believed that the dynamic response of materials can be described by two relaxation times, reflecting the slow and fast change characteristics of materials respectively, they also revealed the impact strain rate effect of epoxy resin and time-temperature equivalence. Haixia et al.²³ used a generalized nonlinear ZWT constitutive model to describe the uniaxial compressive mechanical behavior of propellants at low, medium, and high strain rates. Their analysis showed that at least four Maxwell elements were required in the model to accurately describe the dynamic mechanical properties of rate-dependent materials.

Yang²⁴ proposed a sticky-hyperelastic constitutive model for the high strain rate effect of rubber materials, which can characterize the hyperelastic properties, strain rate correlation as well as history dependence. Xiangrong²⁵ modified the constitutive model proposed by Yang et al., changed the Rivlin function to Yeoh function, and proposed a new nonlinear sticky superelastic constitutive model based on the high strain rate effect. Yuliang²⁶ constructed an improved Ogden model considering the strain rate effect based on the Ogden model by using the strain energy function, the model has good computational accuracy when dealing with large strain data of viscoelastic materials under impact compression. The existing constitutive models suitable for high strain rate can describe the mechanical characteristics of viscoelastic materials during large impact deformation. However, there are too many model parameters, unclear physical significance, and limitations that cannot represent the dynamic mechanical characteristics in the frequency domain of viscoelastic materials.

Under the dynamic service conditions such as variable temperature, frequency conversion and impact, the viscoelastic

damping materials show strong nonlinear properties. However, the traditional integer-order constitutive model fails to accurately characterize the history-dependence and temperature-frequency correlation of viscoelastic materials, as well as the mechanical properties when striking large deformations. The existing viscoelastic constitutive model for high strain rate cannot represent the viscoelastic dynamic mechanical properties in the frequency domain. Fractional-order constitutive models need to improve the accuracy of characterization of viscoelastic dynamic mechanical properties over a wide range of temperatures, frequencies, and strain rates. Previous studies showed that the constant fractional model can accurately describe the dynamic mechanical properties of viscoelastic materials in single stage,^{27,28} while for the characterization of multi-stage dynamic mechanical properties, it has low generalization ability. In other words, the constant fractional model has a large error for the description of the consecutive multiple stages. Based on this, the research takes the value of the order and constructs a constitutive model of distributed order viscoelastic materials to accurately characterize the constitutive mechanical behavior with stage characteristics. It could reveal the dynamic damping properties of viscoelastic materials.

2. THE DISTRIBUTED FRACTIONAL ORDER KELVIN-VOIGT CONSTITUTIVE MODEL

2.1. Model Building

Based on the theory of fractional calculus, from the perspective of phenomenology and the modeling idea of a classical model including component combination, the DFKV is established. The model consists of the elastic element k and the distributed fractional order damping element $\langle c, \alpha_{mi} \rangle$ in parallel, as Figure 1 shows. The total stress of DFKV model of the parallel structure is the sum of an elastic element and a distributed order damping element, as $\sigma = \sigma_e + \sigma_f$, which also obtains, $F_d = \sigma A = \sigma_e A + \sigma_f A$. The total strain is equal to the strain of the elastic element and the distributed order damping element, as $\varepsilon = \varepsilon_e = \varepsilon_f$. Therefore, the parameter of the constitutive operator of the distribution fractional order is $n = 0, m = 1, p_0 = 1, q_0 = k, q_1 = c, \alpha_{0i} = 0, \alpha_{1i} = \alpha_i, \beta_{0j} = 0$. The DFKV constitutive equation is:

$$\sigma = k\varepsilon + cD_t^{\alpha_i}\varepsilon; \tag{1}$$

where:

$$D_t^{\alpha_i} f(t) = \frac{1}{\Gamma(n - \alpha_i)} \int_a^t \frac{f^{(m)}(\tau)}{(t - \tau)^{\alpha_i - m + 1}} d\tau; \tag{2}$$

where $n = [\alpha_i], n - 1 < \alpha_i \leq n$.

The mechanical properties of viscoelastic materials have stage characteristics related to strain, and the typical stress-strain curve can be divided into elastic stage, softening stage and hardening stage (see Figure 2). In the elastic stage I, the stress-strain relationship of the material is close to linear. Within the softening stage II, as the strain increases, the internal temperature of the material increases and softening phenomenon occurs, presenting a hysteretic stress-strain relationship. In the hardening stage III, compared to the softening stage, the slope of the stress-strain curve increases.

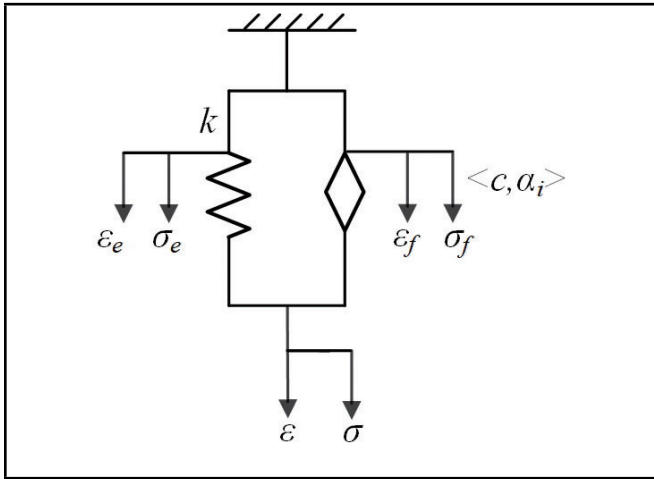


Figure 1. DFKV constitutive model.

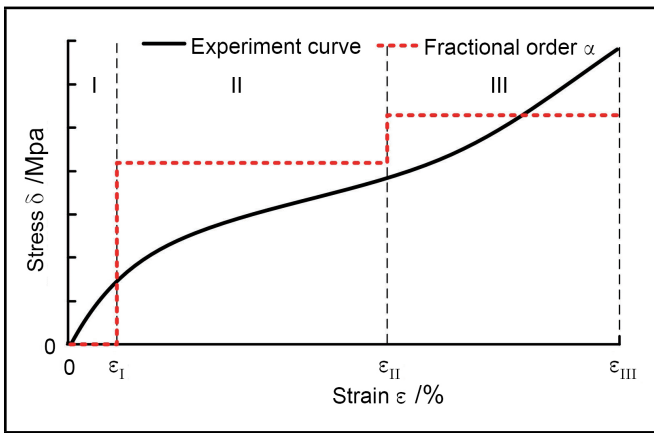


Figure 2. Typical constitutive relation for viscoelastic materials.

To reflect the mapping relationship between the distribution order α_i and the viscoelastic properties, the order α_i is taken as the distribution function to reflect the stage of the dynamic mechanical behavior of viscoelastic materials, as:

$$\alpha_i = \begin{cases} \alpha_1 & 0 \leq \varepsilon < \varepsilon_I \\ \alpha_2 & \varepsilon_I \leq \varepsilon < \varepsilon_{II} \\ \alpha_3 & \varepsilon_{II} \leq \varepsilon < \varepsilon_{III} \end{cases} \quad (3)$$

In particular, when $\alpha_i = 0$, the distributed order viscoelastic element follows Hooker's law, which becomes pure elastic element. When $\alpha_i = 1$, it follows Newton's constant viscosity law, which becomes pure viscoelastic element.

2.2. Verification

With the silicone rubber as the research object, the quasi-static uniaxial tensile test is carried out in the universal material testing machine (Testometric M350-10 kN). Taking the stress-strain curve of 500 mm / min as an example (see Figure 3), the constitutive model parameters of DFKV distribution are identified and analyzed. The model parameters are identified by the least squares method. When $0 \leq \varepsilon < 20\%$, the material is in the pure elastic stage, the stress and strain is a linear relationship, $\alpha_1 = 0$, $k_e = 2.91 \times 10^6$ N/mm. When $20\% \leq \varepsilon < 113.12\%$, the material is in the softening stage, the performance of "visco-elastic co-existence", the stress and strain is a nonlinear relationship, $\alpha_1 = 0.38$, $c = 0.12 \times 10^6$ Ns/mm,

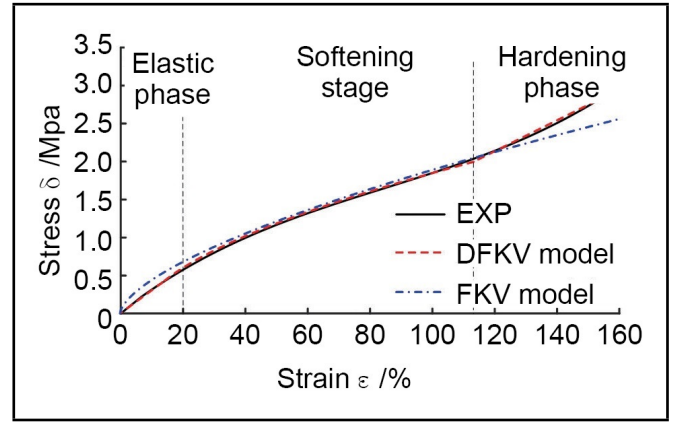


Figure 3. Fitting of the quasi-static experimental curves.

$k = 2.84 \times 10^6$ N/mm. When $113.12 \leq \varepsilon < 160\%$, it is hardening, and it is a non-linear relationship. $\alpha_1 = 0.38$, $c = 0.12 \times 10^6$ Ns/mm, $k = 2.84 \times 10^6$ N/mm. When $113.12 \leq \varepsilon < 160\%$, the material is in the hardening stage, parameter $\alpha_1 = 0$, $k_e = 2.06 \times 10^6$ N/mm.

Root mean square (RMSE) is selected as the error evaluation index, and the specific expression is as follows:

$$RMSE = \sqrt{\frac{1}{n} \sum_{i=1}^n (y_t - y_e)^2}; \quad (4)$$

where, y_t and y_e are the experimental value and theoretical value, respectively.

The fitting error RMSE value of the DFKV model is 0.029, while the constant fractional FKV model is 0.128. It can be seen that the DFKV model has a high fitting accuracy on the silicone rubber quasi-static stress-strain curve, which can accurately describe the quasi-static constitutive mechanical behavior of the viscoelastic material under large deformation conditions.

3. DYNAMIC DAMPING CHARACTERISTIC OF VISCOELASTICITY UNDER FREQUENCY CONVERSION CONDITION

3.1. Analysis of Distributed Order Hysteresis Characteristics

Under simple harmonic excitation, the strain of DFKV model is $\varepsilon(t) = \varepsilon_0 \sin \omega t$. The following equation can be obtained by the definition of the fractional derivative operator:

$$D_t^{\alpha_i} \varepsilon(t) = \varepsilon_0 \omega^{\alpha_i} \sin(\omega t + \alpha_i \pi / 2). \quad (5)$$

According to Equation (5), the DFKV constitutive Equation (1) can be further converted into:

$$\sigma(t) = k \left[1 + \omega^{\alpha_i} \left(\frac{c}{k} \right) \cos \left(\frac{\alpha_i \pi}{2} \right) \right] \varepsilon_0 \sin \omega t + c \omega^{\alpha_i} \sin(\alpha_i \pi / 2) \varepsilon_0 \cos \omega t. \quad (6)$$

When Equation (6) is further rewritten to elliptical type, the hysteresis curve expression of DFKV model under simple har-

monic excitation is obtained:

$$\left\{ \frac{\sigma(t) - k [1 + (c/k)\omega^{\alpha_i} \cos(\alpha_i\pi/2)] \varepsilon(t)}{c\omega^{\alpha_i} \varepsilon_0 \sin(\alpha_i\pi/2)} \right\}^2 + \left[\frac{\varepsilon(t)}{\varepsilon_0} \right]^2 = 1. \tag{7}$$

The formation of viscoelastic hysteresis curve needs to consider the effects of both material viscosity and nonlinear elasticity simultaneously. The larger the viscosity is, the larger the energy dissipation capacity is. In addition, the stress corresponding to the maximum strain decreases with increasing α_i , that is, the material elasticity decreases with increasing α_i . In particular, when $\alpha_i = 0$, the hysteresis loop Equation (7) degenerates to an ideal undamped elastic model, $\sigma(t) = 2k\varepsilon(t)$, which indicates that the stress is proportional to the strain, and under this condition, the corresponding hysteresis loop is a straight line, and there is no energy dissipation. When $\alpha = 1$, Equation (7) degenerate to an ideal stiffness-free Newtonian fluid model, $\sigma(t) = k + (kc/\omega)\dot{\varepsilon}(t)$. The stress is proportional to the first derivative of the strain, corresponding to the largest hysteresis ring area, under this condition, the largest energy consumption occurred.

3.2. Distributed Fractional Order Dynamic Modulus Expressions and Parametric Analysis

The Laplace transform of the DFKV constitutive Equation 1 yields its dynamic complex modulus:

$$E(\omega) = k + c(i\omega)^{\alpha_i}. \tag{8}$$

Due to $i^{\alpha_i} = \cos(\alpha_i\pi/2) + i\sin(\alpha_i\pi/2)$, the dynamic performance coefficients are obtained by separating the real and imaginary parts of the complex modulus:

(1) storage modulus

$$E_d(\omega) = k + c\omega^{\alpha_i} \cos\left(\frac{\alpha_i\pi}{2}\right); \tag{9}$$

(2) loss modulus

$$E_l(\omega) = c\omega^{\alpha_i} \sin\left(\frac{\alpha_i\pi}{2}\right); \tag{10}$$

(3) loss factor

$$\eta(\omega) = \frac{E_l(\omega)}{E_d(\omega)} = \frac{c\omega^{\alpha_i} \sin\left(\frac{\alpha_i\pi}{2}\right)}{k + c\omega^{\alpha_i} \cos\left(\frac{\alpha_i\pi}{2}\right)}. \tag{11}$$

The expressions of the viscoelastic dynamic performance parameters are explicit functions of the constitutive parameters, and their partial derivatives are easy to obtain. Therefore, the analytical method is used to carry out the sensitivity analysis and to discuss the trends and patterns of the influence of the variation of the material's constitutive parameters on the dynamic properties of viscoelastic materials. The sensitivity of the storage modulus E_d , dissipation modulus E_l , and loss factor η of the DFKV model to the order α_i are:

$$L_{E_d, \alpha_i} = c\omega^{\alpha_i} (A \ln \omega - B\pi/2); \tag{12}$$

$$L_{E_l, \alpha_i} = c\omega^{\alpha_i} (B \ln \omega + A\pi/2); \tag{13}$$

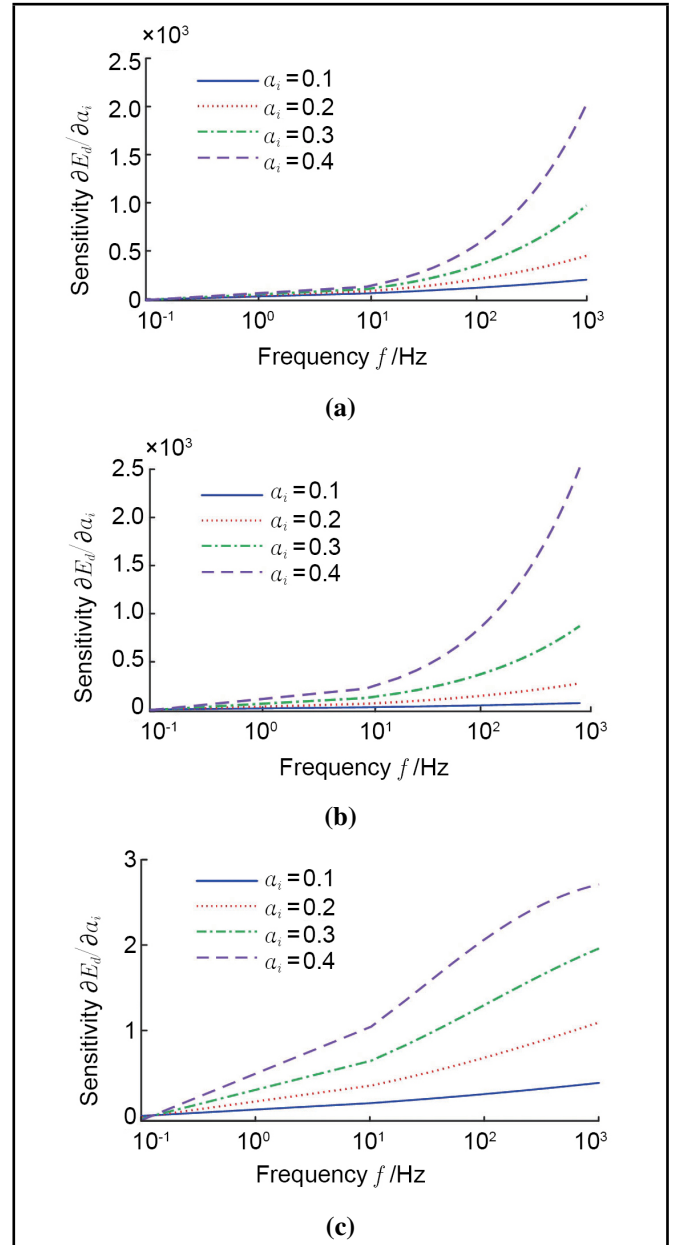


Figure 4. Parameter sensitivity for α_i of DFKV model. (a) Parameter sensitivity for E_d to α_i ; (b) E_l to α_i ; (c) η to α_i .

$$L_{\eta, \alpha_i} = [c\omega^{\alpha_i} (B \ln \omega + A\pi/2) (k + Ac\omega^{\alpha_i}) - Bc^2\omega^{2\alpha_i} (A \ln \omega - B\pi/2)] (k + Ac\omega^{\alpha_i})^{-2}; \tag{14}$$

where $A = \cos(\alpha_i\pi/2)$.

The sensitivity trends of dynamic performance parameters E_d , E_l , and η to order α_i are shown in Figure 4. When order α_i takes the value of 0.1 ~ 0.4, the L_{E_d, α_i} , L_{E_l, α_i} and L_{η, α_i} are all in the positive value, and they are all positively correlated with order α_i , and with the increase of frequency, L_{E_d, α_i} , L_{E_l, α_i} and L_{η, α_i} all show an increasing trend. Among them, in the low-frequency band, L_{E_d, α_i} is less affected by the order α_i . In the high-frequency band, with the increase of the order α_i , L_{E_d, α_i} changes relatively obviously. In contrast, the value of L_{E_l, α_i} is slightly more affected by the order α_i .

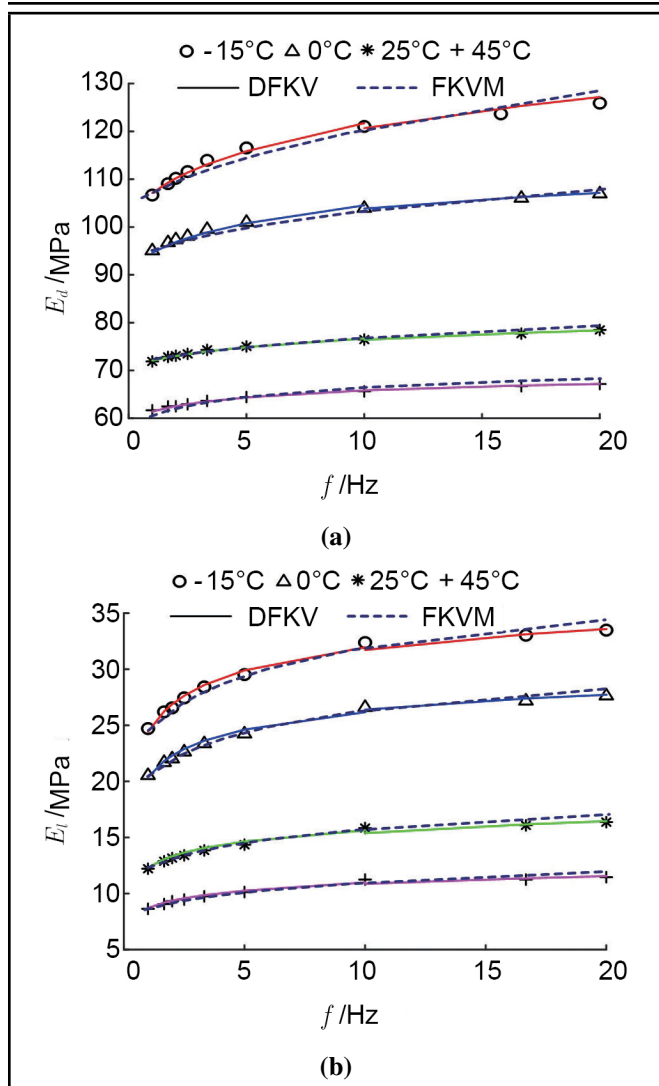


Figure 5. Fitting results of DFKV model DMA experiment. (a) Storage modulus E_d ; (b) Loss modulus E_l .

4. VISCOELASTIC DYNAMIC DAMPING CHARACTERISTICS UNDER VARIABLE TEMPERATURE AND FREQUENCY CONVERSION

The experimental frequency spectrum of DMA for silicone rubber is shown in Figure 5, which shows that the storage modulus E_d , loss modulus E_l and the loss factor η of silicone rubber increase with frequency, and they all tend to be constant. The effect of frequency on the properties of viscoelastic materials is essentially the relationship among the relaxation time of the molecular chains and the time of stress application and observation time. (a) When the frequency f is small, the stress changes slowly and the molecular chain segments have enough time for conformational transformation and untangling or relaxation, which can be regarded as free movement. The values of E_d , E_l , and η are small because γ deformation occurs easily and the slip and friction between chain segments are small. (b) As the frequency f increases, the motion of molecular chain segments gradually cannot catch up with the change of stress, which can be regarded as a finite motion under certain constraints, and the internal dissipation is larger. E_d , E_l , and η all show an increasing trend.

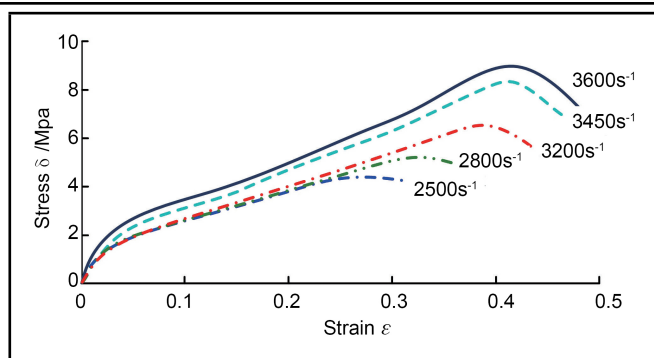


Figure 6. SHPB stress-strain curves for SR.

The DFKV model is used to fit the experimental frequency spectrum of silicone rubber DMA. The fitting results are shown in Figure 5. The model parameters are shown in Table 1. It can be seen that the order α_i corresponding to the frequency $f = 10 \sim 20$ Hz is slightly reduced compared with that of $f = 1 - 10$ Hz. It reflects the tendency of the material's viscosity to weaken and its elasticity to increase. The fitting error RMSE values are shown in Table 2. The fitting error RMSE values of the DFKV model with respect to the storage modulus and loss modulus are lower than those of the FKVM model.

5. VISCOELASTIC DYNAMIC DAMPING CHARACTERISTICS AT HIGH STRAIN RATE

5.1. Damping Characteristics Analysis

A short cylindrical specimen with a diameter of 6.5 mm and a thickness of 3 mm is used to carry out the SHPB impact mechanical properties experiments. The experimental stress-strain curves of silicone rubber at strain rates of 2500 s^{-1} , 2800 s^{-1} , 3200 s^{-1} , 3450 s^{-1} and 3600 s^{-1} are obtained. The filtered experimental curves are shown in Figure 6. The values of the characteristic parameters of the curves are shown in Table 3.

The experimental results of silicone rubber SHPB show that the constitutive mechanical properties of silicone rubber under high strain rate present periodic characteristics with deformation and show obvious strain rate correlation. Among them, the yield strain increased from 0.259 to 0.416, and the yield stress increased from 4.383 MPa to 9.068 MPa. Definition $d\sigma_s/d(\lg\dot{\epsilon})$ characterizes the strain rate correlation of the material yield stress.³⁰ $\sigma_s = A + B \lg(\dot{\epsilon})$ obtained by fitting calculation. Where, A and B both are obtained by fitting calculation, $A = -95.5203$, $B = 29.3305$. The strain rate correlation index of silicone rubber is 29.331. The cut-line modulus E at strain $\epsilon = 0.2$ is used to evaluate the material elasticity. Compared with the value of E at the strain rate of 2500 s^{-1} , the incremental range of the value of E at the other strain rates is 1.65% to 19.

The DFKV model is used to fit the stress-strain curve of silicone rubber at high strain rates. The fitting results of strain rates 2800 s^{-1} and 3450 s^{-1} are shown in Figure 7, and the parameters of each model are shown in Table 4. It can be seen that in the elastic phase, the order $\alpha_1 = 0$, and the k_e value is basically unchanged. Exceptionally, the k_e value increases at strain rate 3600 N/mm . In the softening stage, the up convex

Table 1. Parameters of DFKV model DMA experiment.

T	Storage modulus E_d			Loss modulus E_l		
	$k/(N/mm)$	$c/(N\cdot s/mm)$	α_i	$c/(N\cdot s/mm)$	α_i	f/Hz
-15	90.81	10.70	0.283	128.70	0.104	1 ~ 10
			0.269		0.102	10 ~ 20
0	72.40	18.04	0.141	103.29	0.106	1 ~ 10
			0.139		0.104	10 ~ 20
25	65.72	4.19	0.252	57.97	0.110	1 ~ 10
			0.244		0.108	10 ~ 20
45	55.91	4.00	0.234	36.17	0.121	1 ~ 10
			0.228		0.117	1 ~ 10

Table 2. RMSE of DFKV model.

T	Storage modulus E_d		Loss modulus E_l	
	DFKV	FKVM	DFKV	FKVM
-15	0.594	0.966	0.256	0.343
0	0.397	0.596	0.211	0.255
25	0.158	0.202	0.168	0.237
45	0.145	0.159	0.124	0.274

Table 3. Parameters of stress-strain curves for SR.

$\dot{\epsilon}/s^{-1}$	2500	2800	3200	3450	3600
ϵ_s	0.259	0.323	0.385	0.415	0.416
σ_s/MPa	4.383	5.437	6.830	8.322	9.068
E/MPa	18.837	19.147	20.155	21.938	22.481

curvature of the curves increases with increasing strain rate. The order α_2 shows an overall increasing trend with increasing strain rate. The hardening stage occurs when the strain rates are $3200 s^{-1}$, $3450 s^{-1}$, and $3600 s^{-1}$, at which time $\alpha_3 = 0$. The material can hardly provide damping energy dissipation in this stage. The k_e value increases with the strain rate, which means the more significant hardening effect.

5.2. Comparative Analysis of Models

The ZWT model and the Ogden model considering the strain rate effect are typical viscoelastic constitutive models for high strain rate conditions. The above two models and the constant-order FKVM model are used to fit the SHPB stress-strain experimental curves of the silicone rubber respectively. The fitting results are shown in Figure 8.

The RMSE values of the fitting errors for the above model are shown in Table 5. At strain rates of $2500 s^{-1}$ and $2800 s^{-1}$, the distribution order model DFKV has the highest fitting accuracy, followed by the FKVM with ZWT model, and the Ogden model is the lowest. At strain rates of $3000 s^{-1}$, $3200 s^{-1}$ and $3450 s^{-1}$, the fitting accuracy of the distributed order model DFKV is highest, the ZWT model takes second and the Ogden model and FKVM model is relatively lowest. Additionally, the order α_i of the distributed order constitutive model can reflect the viscoelastic distribution during impact deformation of viscoelastic materials, which has fewer parameters and clearer physical meaning.

6. CONCLUSION

- (1) Based on the fractional calculus and viscoelasticity theory, the DFKV constitutive model is established by considering the stage characteristics of the deformation development of viscoelastic materials. The accuracy of the

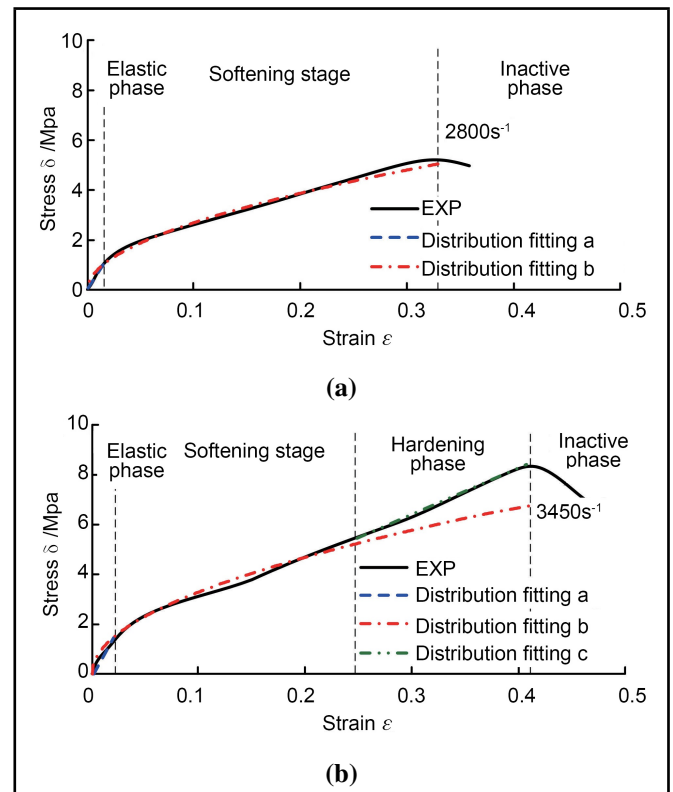


Figure 7. Fitting results of DFKV model for SHPB experiment. (a) Strain rate $2800 s^{-1}$; (b) Strain rate $3450 s^{-1}$.

DFKV model is verified by quasi-static tensile experiments.

- (2) Distributed-order dynamic modulus expressions were derived, and model parameter characterization were carried out, indicating that the order α_i of the DFKV model was positively correlated with the storage modulus, loss modulus and loss factor. On the DMA experimental platform, the variable frequency conversion dynamic mechanical property experiments of silicone rubber were completed. The results show that the corresponding order α_i at the frequency $f = 10 \sim 20 Hz$ is slightly reduced compared with that at $f = 1 \sim 10 Hz$, reflecting the tendency of the material viscosity weakening and elasticity increasing.
- (3) Experiments on the impact mechanical properties of silicone rubber SHPB was carried out to characterize the macroscopic deformation behavior of the material according to the damping dissipation mechanism. The obvious strain rate correlation of the viscoelastic damping material was revealed, and its strain rate effect index is 29.331. It also had the stage characteristics related to the strain, and

Table 4. Parameters of DFKV model SHPB experiment.

$\dot{\epsilon}/s^{-1}$	Elastic stage		Softening stage	Hardening stage	
	α_1	$k_e \times 10^7$ /(N/mm)	c, k	α_2	α_3 $k_e \times 10^7$ /(N/mm)
2500	0	7.239	$c = 1.4 \times 10^5, k = 1 \times 10^6$	0.495	—
2800		7.239		0.497	—
3200		7.239		0.493	1.370
3450		7.239		0.509	1.603
3600		10.41		0.512	2.004

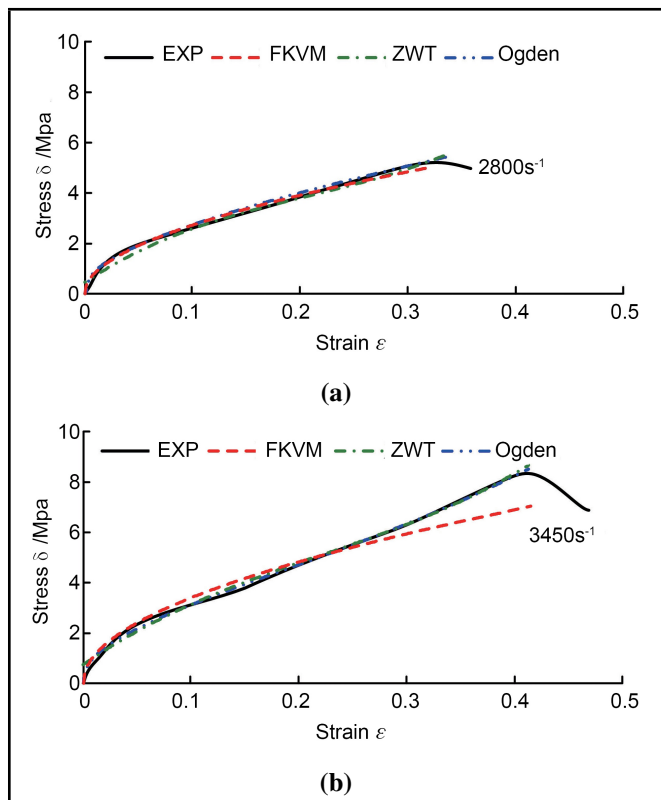


Figure 8. Fitting results of models. (a) Strain rate 2800 s^{-1} ; (b) Strain rate 3450 s^{-1} .

Table 5. RMSE of different models.

$\dot{\epsilon}/s^{-1}$	DFKV	FKVM	ZWT	Ogden
2500	0.058	0.064	0.111	0.261
2800	0.142	0.143	0.132	0.227
3000	0.068	0.283	0.125	0.248
3200	0.135	0.578	0.157	0.225
3450	0.135	0.567	0.199	0.287

the order in the DFKV model was reflected by the above characteristics.

- (4) The RMSE values of the distributed fractional order DFKV constitutive model are smaller than those of the existing comparative models. This reflects the “elastic-resistive co-existence” of viscoelastic materials., Additionally, the physical significance of the parameters is clear, so that it can accurately characterize the viscoelastic dynamic mechanical properties in a wider frequency domain and under different strain rates.

ACKNOWLEDGEMENTS

This work was supported by the National Natural Science Foundation of China [52302475], Fundamental Research Program of Shanxi Province [20210302124444] [202203021212317], Scientific and Technological Innovation Programs of Higher Education Institutions in Shanxi [2022L319][2022L303], Taiyuan University of Science and Technology Scientific Research Initial Funding [20222093].

REFERENCES

- Araujo, G.P Donadon, Salerno, G., Cássia, R., and Sales, M. Temperature effects on the mechanical behaviour of PAEK thermoplastic composites subjected to high strain rates under compression loading, *Composite Structures*, **261**(01), 113299, (2021). <https://doi.org/10.1016/j.compstruct.2020.113299>
- Amabili, M., Balasubramanian, P, and Ferrari, G. Nonlinear vibrations and damping of fractional viscoelastic rectangular plates, *Nonlinear Dynamics*, **103**(4), 3581–3609, (2021). <https://doi.org/10.1007/s11071-020-05892-0>
- Shi, C., Cao, C., Lei, M., Peng, L., and Shen, J. Time-dependent performance and constitutive model of EPDM rubber gasket used for tunnel segment joints, *Tunnelling and Underground Space Technology*, **50**(490–498), (2015). <https://doi.org/10.1016/j.tust.2015.09.004>
- Ebrahimi, F., Hamed, S. Hossrini, S., and Selvamani, R. Thermo-electro-elastic nonlinear stability analysis of viscoelastic double-piezo nanoplates under magnetic field, *Structural Engineering and Mechanics*, **73**(5), 565–584, (2020). <https://doi.org/10.12989/sem.2020.73.5.565>
- Zhu. H.P and Xu. Y.L. Optimum parameters of Maxwell model-defined dampers used to link adjacent structures, *Journal of Sound & Vibration*, **279**(1–2), 253–274, (2005). <https://doi.org/10.1016/j.jsv.2003.10.035>
- Sharma, A.K, Datta, R., Agarwal, S., and Bhattacharya, B. Displacement transmissibility based system identification for polydimethylsiloxane integrating a combination of mechanical modelling with evolutionary multi-objective optimization, *Engineering Optimization*, **52**(6), 1037–1051, (2019). <https://doi.org/10.1080/0305215X.2019.1634701>
- Lindner, M. et al. The transition from purely elastic to viscoelastic behavior of silica optical fibers at high temperatures characterized using regenerated Bragg gratings, *Optics Express*, **28**(5), 7323–7340, (2020). <https://doi.org/10.1364/OE.384402>

- ⁸ Nutting P.G. A new general law of deformation, *Journal of the Franklin Institute*, **191**(5), 679–685, (1921). [https://doi.org/10.1016/S0016-0032\(21\)90171-6](https://doi.org/10.1016/S0016-0032(21)90171-6)
- ⁹ Gemant, A. A method of analyzing experimental results obtained from elastic-viscous bodies, *Physics*, **7**(8), 311–317, (1936). <https://doi.org/10.1063/1.1745400>
- ¹⁰ Koeller, R.C. A theory relating creep and relaxation for linear materials with memory, *Journal of Applied Mechanics*, **77**(3), 448–452, (2010). <https://doi.org/10.1115/1.4000415>
- ¹¹ Müller S, K'astner M, Brummund, J., and Ulbricht, V. On the numerical handling of fractional viscoelastic material models in a FE analysis, *Computational Mechanics*, **51**(6), 999–1012, (2013). <https://doi.org/10.1007/s00466-012-0783-x>
- ¹² Khajehsaeid, H. A comparison between fractional-order and integer-order differential finite deformation viscoelastic models: Effects of filler content and loading rate on material parameters, *International Journal of Applied Mechanics*, **10**(2018). <https://doi.org/10.1142/S1758825118500990>
- ¹³ Jiaguo, L. The Complex Modulus and The Complex Compliance for Higher-order Fractional Constitutive Models of Visco-elastic Materials, *Journal of Shandong University, Natural Science*, **2008**(4), 85–88.
- ¹⁴ Yongling, Z. Vibration Isolation Rubber Characterization and Rubber Suspension Structural Optimization, BeiJing, Tsinghua University, (2016).
- ¹⁵ Mingyu, X. and Wenchang, T. Generalized Fractional Cell Network Formulation and Its Generalized Solution of the Constitutive Equations for Viscoelastic Materials, *Science in China (Series A)*, **32**(8), 673–681, (2002).
- ¹⁶ Londoño, O.G, Paulion, G.H, and Buttlar, W.G. Fractional calculus derivation of a rate-dependent PPR-based cohesive fracture model: theory, implementation, and numerical results, *International Journal of Fracture*, **216**(2019), 1–29. <https://doi.org/10.1007/s10704-018-00334-w>
- ¹⁷ Wang, B. and Kari, L. A nonlinear constitutive model by spring, fractional derivative and modified bounding surface model to represent the amplitude, frequency and the magnetic dependency for Magneto-sensitive rubber, *Journal of Sound and Vibration*, **438** (2019), 344–352. <https://doi.org/10.1016/j.jsv.2018.09.028>
- ¹⁸ Xiao, X., Shiqiao, G., and Dongmei, Z. Mechanical behavior of liquid nitrile rubber-modified epoxy resin: Experiments, constitutive model and application International, *Journal of Mechanical Sciences*, **151**, (2019), 46–60. <https://doi.org/10.1016/j.ijmecsci.2018.11.003>
- ¹⁹ Golewski, P, Sadowski, T., and Rusinek, A. The SHPB tests for GFRP composites subjected to three levels of strain rates, *Materials Today: Proceedings*, **45**(5), 4275–4279, (2021). <https://doi.org/10.1016/J.MATPR.2020.12.512>
- ²⁰ Brizard, D., Ronel, S., and Jacquelin, E. Correction to: Estimating Measurement Uncertainty on Stress-Strain Curves from SHPB, *Experimental Mechanics*, **61**(1065), 1065, (2021). <https://doi.org/10.1007/S11340-021-00702-Z>
- ²¹ Shisheng, H., Zhengdao, W., and Lizhong, Z. Experimental Study of Dynamic Mechanical Behaviors of Silicone Rubber Foam, *Polymeric Materials Science & cboxEngineering*, **15**(2), 113–115, (1999). <https://doi.org/10.16865/j.cnki.1000-7555.1999.02.032>
- ²² Shisheng, H., et al. Review of The Development of Hopkinson Pressure Bar Technique in China, *Explosion and Shock Waves*, **34**(6), 641–657, (2014). [https://doi.org/10.11883/1001-1455\(2014\)06-0641-17](https://doi.org/10.11883/1001-1455(2014)06-0641-17)
- ²³ Haixian, Z. et al. Research on The Viscoelastic Constitutive Model of HTPB Propellant Over A Wide Range of Strain Rates, *Journal of Solid Rocket Technology*, **40**(3), 325–329, (2017). <https://doi.org/10.7673/j.issn.1006-2793.2017.03.010>
- ²⁴ Yang, L.W, Shim, V.P.W, Lim, C.T. A visco-hyperlastic approach to modeling the constitutive behavior of rubber, *International Journal of Impact Engineering*, **24**(6–7), 545–560, (2000). [https://doi.org/10.1016/S0734-743X\(99\)00044-5](https://doi.org/10.1016/S0734-743X(99)00044-5)
- ²⁵ Xiangrong, Z., Qiang,W., and Baozheng, W. A Nonlinear Visco-Hyperelastic Constitutive Model Based on Yeoh Strain Energy Function with Its Application to Impact Simulation, *Journal of Vibration and Shock*, **26**(5), 33–37, (2007). <https://doi.org/10.1017/S0022215100091155>
- ²⁶ Yuliang, L., Fangyun, L., and Li, L. Constitutive Behaviors of a Silicone Rubber at High Strain Rates, *Chinese Journal of High Pressure Physics*, **2007**(3), 289–294. <https://doi.org/10.1051/jp4:2006134047>
- ²⁷ Zhanlong, L. et al. Fractional Maxwell model of viscoelastic oscillator and its frequency response, *Journal of Vibration Engineering & Technologies*, **6**, 5, 1–6, (2018). <https://doi.org/10.1007/s42417-018-0005-8>
- ²⁸ Ciniello, A.P.D, Bavastri, C.A, and Pereira, J.T. Identifying Mechanical Properties of Viscoelastic Materials in Time Domain Using the Fractional Zener Model, *Latin American Journal of Solids & Structures*, **14**(1), 131–152, (2017). <https://doi.org/10.1590/1679-78252814>
- ²⁹ Jiménez, L.M., Cruz-Duarte, J.M., Escalante-Martínez, J.E., and Rosales-García, J.J.. Analytical and experimental study for mechanical vibrations of a two-coupled spring masses system via Caputo-based derivatives, *Mathematical Methods in the Applied Sciences*, **47**(5), 1–19, (2021). <https://doi.org/10.1002/mma.7421>
- ³⁰ Pingsheng, H. *Mechanical Properties of polymers*, University of Science and Technology of China Press, HeFei, (2008).